

# X-Ray and Raman Investigations on Cyanides of Mono- and Divalent Metals and Synthesis, Crystal Structure and Raman Spectrum of $\text{Tl}_5(\text{CO}_3)_2(\text{CN})$

Olaf Reckeweg and Arndt Simon

Max-Planck-Institut für Festkörperforschung, D-70569 Stuttgart

Reprint requests to Dr. O. Reckeweg or Prof. Dr. Dr. h. c. mult. A. Simon.

Fax: +49(0)711 6 89 - 1642. E-mail: olaf.reykjavik@gmx.de

Z. Naturforsch. **57 b**, 895–900 (2002); received April 10, 2002

Carbonate, Cyanide, Raman Spectroscopy

Pseudobinary cyanides of monovalent and divalent metals were synthesized, and X-ray and Raman data of the cyanides were measured. Single crystal X-ray structure analyses were performed on  $\text{Zn}(\text{CN})_2$  ( $Pn\bar{3}m$  (No. 224),  $a = 591.32(7)$  pm),  $\text{Hg}(\text{CN})_2$  ( $I\bar{4}2d$  (No. 122),  $a = 969.22(14)$  and  $c = 890.15(18)$  pm) and for the first time on  $\text{AgCN}$  ( $I\bar{4}2d$  (No. 166),  $a = 600.58(8)$  and  $c = 526.28(11)$  pm). The data are compared with literature data. The reaction of TlF and NaCN in 25% aqueous ammonia solution in air led to  $\text{Tl}_5(\text{CO}_3)_2(\text{CN})$  which was characterized by X-ray ( $Cmca$  (No. 64), 1468.1(3), 1171.6(2) and 1266.0(3) pm) and Raman spectroscopy.

## Introduction

The crystal structures and properties of most binary cyanides of monovalent metals are known because of the extensive use of cyanides in chemical research and industrial applications. It is one of many known facts about ionic cyanides like TICN that HCN is set free if the compound is exposed to air. This is due to the formation of the respective carbonate by the uptake of  $\text{CO}_2$  from the atmosphere. We report here the crystal structure and the Raman data of  $\text{Tl}_5(\text{CO}_3)_2(\text{CN})$ , an intermediate on the reaction path from TICN to  $\text{Tl}_2\text{CO}_3$ . Furthermore, we give a survey of X-ray and Raman spectroscopic data for pseudobinary cyanides of mono- and divalent metals collected by us and from literature.

## Experimental Section

ACN ( $A = \text{Na}, \text{K}, \text{Cu}, \text{Ag}$ )

NaCN (Merck, p. a.), KCN (Merck, reinst), CuCN (Aldrich, 99.99%), and AgCN (Aldrich, 99%) were commercially available and used as received. All powders were colorless, CuCN showed a faint greenish and AgCN a pinkish tint. The AgCN powder was recrystallized from 25 % aqueous ammonia solution (Merck, p. a.) to obtain single crystals.

RbCN and CsCN

1.05 g RbF (Strem, 99 %) or 1.52 g of CsF (Fluka,  $\geq 99\%$ ) and 0.5 g NaCN were dissolved each in 4 ml of

degassed  $\text{H}_2\text{O}$  at 80 °C. Upon mixing the fluoride and the cyanide solution, a white slurry of NaF precipitated. After one day at 4 °C, the NaF was filtered off and washed with 10 ml of ice-cold ethanol. The ethanol-water mixture was evaporated and the white residue was identified as pure RbCN (0.8 g, 71% yield) or CsCN (1.1 g, 69% yield), respectively, according to their respective X-ray powder pattern.

AuCN

0.5 g of Au powder (Strem, 99.9%) was dissolved in 20 ml of a boiling aqueous solution of 150 mg NaCN in air. After acidifying the solution with conc.  $\text{HNO}_3$ , a yellow precipitate formed immediately which was filtered off, washed with ice-cold ethanol and dried at 80 °C (0.52 g, 92% yield). Gold was detected in the powder diffractogram with an intensity of 1.3%  $I_{\text{max}}$  for 111.

TICN

1.75 g of TlF and 0.51 g of KCN were dissolved each in 5 ml of degassed water at 80 °C. A white precipitate formed immediately upon mixing the solutions. After keeping the liquor at 80 °C for 2 h, the closed reaction vessel was kept at 4 °C for 1 d to allow the crystallization to complete. The white powder started to turn pinkish, but gave no indication for decomposition. The precipitate was filtered off, washed with ice-cold ethanol and dried under vacuum (1.52 g, 84% yield).

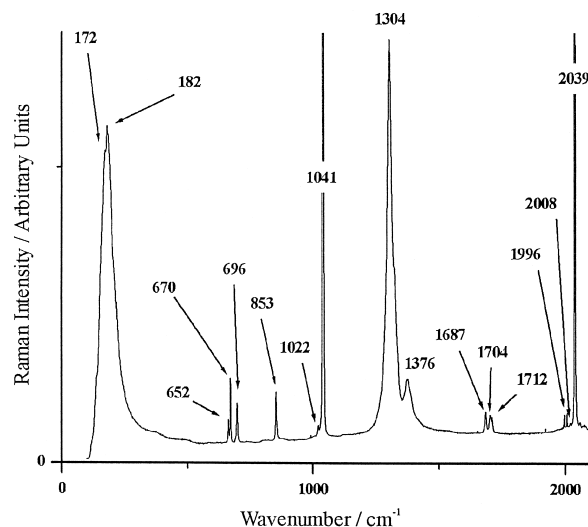


Fig. 1. Raman Spectrum of  $Tl_5(CO_3)_2(CN)$ . The two broad peaks at 1304 and 1376  $cm^{-1}$  are attributed to the grease used during the preparation of the crystals. They probably cover up one of the vibrational modes of  $CO_3^{2-}$ .

#### $M(CN)_2$ ( $M = Zn, Cd, Hg$ )

1.52 g of  $Zn(NO_3)_2 \cdot 6H_2O$  or 1.57 g of  $Cd(NO_3)_2 \cdot 4H_2O$ , respectively, were treated with 0.5 g of NaCN in the same manner and under the same conditions as described for RbCN. Colorless and transparent, octahedral aggregates of  $M(CN)_2$  started to form immediately after mixing the solutions ( $Zn(CN)_2$ : 0.47 g, 78% yield;  $Cd(CN)_2$ : 0.61 g, 73% yield).  $Hg(CN)_2$  (Aldrich, 99%) was recrystallized from 25% aqueous ammonia.

#### $Tl_5(CO_3)_2(CN)$ (3)

500 mg of TlF (Strem, 99%) and 110 mg of NaCN were dissolved in 50 ml of a 25% aqueous ammonia solution to yield a transparent, colorless solution. Transparent crystals with a grey shade started to form after a week under normal atmospheric conditions just below the surface of the solution as irregular polyhedra. The crystals were stable even when removed from the mother liquor.

#### X-Ray and Raman Investigations

The X-ray powder diffractograms were taken on a Stoe powder diffractometer to confirm the identity of the products. The diffractograms of the compounds were indexed and refined with the program WinXPOW [1].

Crystals suitable for X-ray diffraction studies were selected under a polarization microscope and

Table 1. Raman frequencies of  $Tl_5(CO_3)_2(CN)$  and assigned modes.

Raman frequencies / $cm^{-1}$	Assigned mode
2039 / 2008 / 1996	$\nu_{symm}(C\equiv N)$
1712 / 1704 / 1687	$\nu_{asymm}(CO_3^{2-})$ ??
1376 / 1304	Grease
1041 / 1022	$\nu_{symm}(CO_3^{2-})$
853	$\gamma(CO_3^{2-})$
696 / 670 / 652	$\delta(CO_3^{2-})$
182 / 172	lattice vibrations

enclosed in thin-walled glass capillaries. Intensity data sets of these specimen were taken on a Stoe IPDS single crystal diffractometer, respectively, and used to solve and refine the crystal structures with the SHELX-TL program suite [2]. Raman investigations were performed on a microscope laser Raman spectrometer (Jobin Yvon, 4 mW, equipped with an HeNe laser with an excitation line at  $\lambda = 632.817$  nm, 20 - 50 $\times$  magnification, samples in quartz glass capillaries, 5 - 200 s accumulation time) on the very specimen used for both single crystal and X-ray powder measurements. The Raman spectrum for  $Tl_5(CO_3)_2(CN)$  is shown in Fig. 1, the frequencies and their assignment are listed in Table 1.

Semi-qualitative analyses with a Tescan 5130 MM electron microscope were performed on  $Tl_5(CO_3)_2(CN)$ , and the only metal found in the analyses was Tl. Selected results of these measurements are displayed in Tables 2 - 4.

Further details of the crystal structure investigations can be obtained from the Fachinformationszentrum Karlsruhe, D-76344 Eggenstein-Leopoldshafen, Germany (fax: +49(0)7247-808-666; e-mail: crysdata@fiz-karlsruhe.de), on quoting the depository number CSD-412316 ( $Tl_5(CO_3)_2(CN)$ ), CSD-412317 ( $Zn(CN)_2$ ), CSD-412315 ( $Hg(CN)_2$ ) and CSD-412417 ( $AgCN$ ).

#### Description of the Crystal Structures

The room temperature X-ray powder diffractograms of NaCN, KCN and RbCN were indexed and refined on the basis of a cubic face centered cell (isotypic to NaCl). The powder diagrams of CsCN and TlCN were indexed and refined on the basis of a primitive cubic cell (isotypic to CsCl). In both cases the cyanide anion is disordered on the chloride position in the respective isotypic structure. The results

Table 2. Results of the X-ray single crystal diffraction work on  $Tl_5(CO_3)_2(CN)$  (**1**),  $Zn(CN)_2$  (**2**),  $Hg(CN)_2$  (**3**) and  $AgCN$  (**4**).

Compound	<b>1</b>	<b>2</b>	<b>3</b>	<b>4</b>
Space group (No.), Z	<i>Cmca</i> (64), 4	<i>Pn<math>\bar{3}m</math></i> (224), 2	<i>I<math>\bar{4}2d</math></i> (122), 8	<i>R<math>\bar{3}m</math></i> (166), 3
CSD-Number	412316	412317	412315	412417
Lattice constants <i>a</i> [pm]	1468.1(3)	591.32(7)	969.22(14)	600.58(8)
<i>b</i> [pm]	1171.6(2)	<i>a</i>	<i>a</i>	<i>a</i>
<i>c</i> [pm]	1266.0(3)	<i>a</i>	890.15(18)	526.28(11)
Calcd density [gcm <sup>-3</sup> ]	7.125	1.886	4.013	4.057
Crystal colour and shape	transparent, colorless Polyhedron	transparent, colorless Polyhedron	transparent, colorless Block	transparent, hexagonal Plate
Crystal size [mm <sup>3</sup> ]	0.12×0.14×0.15	0.15×0.15×0.15	0.12×0.18×0.28	0.03×0.03×0.01
Diffractometer	Stoe IPDS	Stoe IPDS	Stoe IPDS	Stoe IPDS
Radiation	Ag-K $\alpha$ ( $\lambda$ = 56.086 pm)	— Mo-K $\alpha$ ( $\lambda$ = 71.073 pm) —		
Ranges [ $2\theta_{max}$ ]; <i>h, k, l</i>	50°; $\pm 21, \pm 17, \pm 19$	66°; $\pm 9, \pm 9, \pm 9$	62°; $\pm 14, -14$ $\rightarrow 12, -11 \rightarrow 12$	60.8°; $\pm 8, -7$ $\rightarrow 8, -6 \rightarrow 7$
Dist. Det.-Crystal [mm]	60	60	80	80
Increments $\Delta\phi$ [°]	1.0	1.0	0.8	1.0
Read imaging plates	220	180	225	180
Exposure time [min]	15	8	3	6
Absorption correction	LP, semi-empirical correction (XPREP [2])	LP	— LP, Num. correction — — (X-SHAPE [3]) —	
$\mu$ [mm <sup>-1</sup> ]	40.28	5.73	12.75	8.74
Transmission: min./max.	0.031 / 0.076	—	0.1434 / 0.4541	0.2392 / 0.6714
Flack-parameter	—	—	0.04(7)	—
Reflections:				
Read; indep.; $F_o > 4\sigma(F_o)$	23920, 1999, 1584	9859; 89; 87	5163; 663; 652	589; 128; 120
$R_{int}$	0.0551	0.0609	0.1136	0.065
Refined parameters	77	6	25	7
$R1; wR2; GooF$ (all refl.)	0.039; 0.058; 1.04	0.018; 0.030; 1.32	0.033; 0.085; 1.10	0.026, 0.069, 1.25
Max. shift / esd, last Refinement cycle	< 0.001	< 0.0005	< 0.0005	< 0.0005
Res. electron dens.: max; min	1.66; $-1.25 e^- / \text{\AA}^3$ 85 pm to Tl3	0.15; $-0.09 e^- / \text{\AA}^3$ 256 pm to Zn	1.92; $-1.70 e^- / \text{\AA}^3$ 93 pm to Hg	0.42; $-0.28 e^- / \text{\AA}^3$ 81 pm to Ag

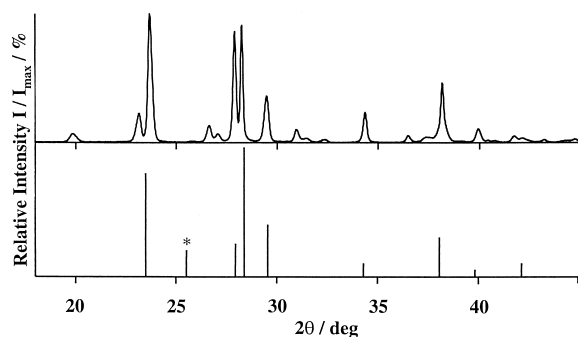


Fig. 2. X-Ray powder diffractogram of CuCN and a bar representation of the literature diffractogram.

of the X-Ray powder investigations are displayed in Table 5.

There is not much known about the structure of CuCN except that it was deduced from extensive

NMR experiments [4] that the structure contains linear chains with ‘head-tail’ disordered cyanide anions. Fig. 2 shows the X-ray powder pattern which indicates that the structure does not have high symmetry. For comparison the powder patterns reported earlier and indexed with orthorhombic lattice parameters [5] is also displayed.

Except for one peak marked with an asterisk in Fig. 2 the patterns are quite similar, the main difference being the better resolution of our measurement. An explanation for the deviations in the powder diffractograms might be our observation that the resolution of the powder pattern decreases if CuCN is exposed to humidity and light over a prolonged period of time. The resolution we achieved by X-ray methods was still not sufficient to index the powder diagram and to refine the structure. DTA / TG results on CuCN showed endothermic effects at

Compound	Atom	Wyckoff site	$x/a$	$y/b$	$z/c$	$U_{eq}$ [pm <sup>2</sup> ]	
Tl <sub>5</sub> (CO <sub>3</sub> ) <sub>2</sub> (CN)	Tl1	16g	0.34186(2)	0.15247(2)	0.52192(2)	300(1)	
	Tl2	16g	0.15536(2)	-0.01053(2)	0.65522(2)	316(1)	
	Tl3	8f	1/2	0.25736(3)	0.78822(3)	357(1)	
	O1	16g	0.4230(4)	0.3443(4)	0.4840(4)	329(11)	
	O2	8f	0	-0.0880(6)	0.6215(6)	312(14)	
	O3	8f	1/2	0.1145(6)	0.5846(6)	313(15)	
	O4	16g	0.0759(4)	-0.0334(2)	0.8492(5)	375(12)	
	C1	8f	0	-0.1336(7)	0.5283(8)	241(16)	
	C2	8f	1/2	0.0149(8)	0.6285(8)	259(18)	
	C/N	16g	0.2827(8)	0.2546(8)	0.7291(8)	589(26)	
	Zn(CN) <sub>2</sub>	Zn	2a	1/4	1/4	1/4	510(3)
		C/N	8e	0.0559(2)	1/2 - x	x	604(5)
AgCN	Ag	3a	0	0	0	882(6)	
	C/N	6c	0	0	0.3943(18)	729(15)	
Hg(CN) <sub>2</sub>	Hg	8d	0.21203(4)	1/4	1/8	386(2)	
	C	16e	0.2035(14)	-0.0729(11)	0.1785(11)	667(34)	
	N	16e	0.2050(11)	0.0464(10)	0.1639(9)	422(17)	

Table 3. Crystal coordinates and equivalent displacement factors<sup>a</sup> of the investigated compounds.

<sup>a</sup>  $U_{eq}$  is defined as a third of the trace of the orthogonalized  $U_{ij}$ -tensor.

Compound	Atoms1	Atoms2	d [pm]	Atoms1	Atoms2	d [pm]
Zn(CN) <sub>2</sub>	4× Zn	C/N	198.8(2)	C	N	114.4(4)
Hg(CN) <sub>2</sub>	2× Hg	C	200.4(10)	2×	N	275.8(10)
	2×	N	305.3(11)	2×	N	316.6(11)
		C	116.4(14)			
AgCN	2× Ag	C/N	207.5(9)	1× C	N	111.2(19)
Tl <sub>5</sub> (CO <sub>3</sub> ) <sub>2</sub> (CN)	1× Tl1	O3	249.4(3)	1×	O1	258.8(5)
	1×	O4	286.0(6)	1×	O4	297.7(6)
	1×	(CN)	301.1(10)	1× Tl2	O2	249.2(3)
	1×	O4	273.2(6)	1×	O1	286.7(5)
	1×	O1	298.6(6)	2× (CN)		304.6(9)
	1× Tl3	O2	278.1(8)	2×	O4	280.1(6)
	2×	O1	297.3(6)	1×	O3	307.4(8)
	1×	(CN)	327.7(12)	2× C1	O1	128.9(7)
	1×	O2	129.6(12)	1× C2	O3	129.2(11)
	2×	O4	128.2(7)	1× C	N	110(2)
	2×	Tl1	301.6(10)	2×	Tl2	304.6(9)
	2×	Tl3	327.7(12)			

Table 4. Selected distances in the structures of the cyanides.

292 °C and at 477 °C with virtually no mass loss in the first case and 23% loss in the second step. These results are in good agreement with the reported decomposition temperature of 473 °C [5]. The Raman experiments gave the symmetric stretching mode at 2172 cm<sup>-1</sup> which is matching literature data (2169 [6] and 2173 cm<sup>-1</sup> [4]). DTA / TG and Raman results gave us no indication for the presence of water contained in the compound.

For AgCN we report the first single crystal structure analysis. Our data yielded a significantly better refinement in the centrosymmetric space group  $R\bar{3}m$  than in the acentric space group  $R3m$ . The same choice was made recently on the basis of total a neu-

tron reflection analysis [7]. The structure itself consists of linear -Ag-X≡X-Ag- chains (X stands for disordered C/N) where the cyanide anion also shows a ‘head-tail’ disorder. Each chain is surrounded by six other chains which are shifted against each other by 1/3 c. The closest Ag-Ag contact is 388.3 pm.

AuCN has a similar structure as AgCN, *i. e.* linear polymeric -Au-X≡X-Au- chains probably also with a ‘head-tail’ disorder, however, without relative shift of the chains. The Au atoms form 2D close packed layers which are held together by the cyanide anions. The closest Au-Au contact is 339.6 pm (Fig. 3b).

Table 5. Spectroscopic and crystallographic data of selected cyanides.

Compound	Space group	<i>a</i> / <i>b</i> / <i>c</i> [pm]	$\nu(\text{C}\equiv\text{N})$ [ $\text{cm}^{-1}$ ]	<i>d</i> (C≡N) [pm]	Ref.
LiCN	<i>Pnma</i>	875 / 374 / 674	2108		[10]
NaCN	<i>Fm<math>\bar{3}m</math></i>	590.16(10)	2089		this work
KCN	<i>Fm<math>\bar{3}m</math></i>	653.92(11)	2077		this work
RbCN	<i>Fm<math>\bar{3}m</math></i>	683.93(10)	2071		this work
CsCN	<i>Pm<math>\bar{3}m</math></i>	427.28(9)	2065		this work
TlCN	<i>Pm<math>\bar{3}m</math></i>	400.5(3)	2049		this work
Be(CN) <sub>2</sub>	<i>Pn<math>\bar{3}m</math></i>	533.9	2233 / 756	118.7	[11]
Mg(CN) <sub>2</sub>	<i>Pn<math>\bar{3}m</math></i>	612.2	2197 / 492	108.5	[11]
Al(CN) <sub>3</sub>	<i>Pm<math>\bar{3}m</math></i>	520.5	2220 / 530	116.4	[11]
Ga(CN) <sub>3</sub>	<i>Pm<math>\bar{3}m</math></i>	529.5	2215 / 440	114.8	[12]
In(CN) <sub>3</sub>	<i>Pm<math>\bar{3}m</math></i>	562.7	2200 / 415	112.5	[13]
Tl(CN) <sub>2</sub>	<i>Pn<math>\bar{3}m</math></i>	666.0	2209 / 2198	?	[11]
Zn(CN) <sub>2</sub>	<i>Pn<math>\bar{3}m</math></i>	590.02	–	118.97	[8, 12]
Cd(CN) <sub>2</sub>	<i>Pn<math>\bar{3}m</math></i>	630.01	–	116.2	[8]
CuCN	<i>mmmB symmetry*</i>	1279 / 1814 / 782*	2172	–	this work
AgCN	<i>R<math>\bar{3}m</math></i>	602.0(7) / 526.4(2)	2169	111(2)	this work
AuCN	<i>P6/mmm</i>	340.5(4) / 509.5(4)	2240	–	this work
Zn(CN) <sub>2</sub>	<i>Pn<math>\bar{3}m</math></i>	590.8(2)	2221	114.4(4)	this work
Cd(CN) <sub>2</sub>	<i>Pn<math>\bar{3}m</math></i>	632.5(3)	2200	–	this work
Hg(CN) <sub>2</sub>	<i>I<math>\bar{4}2d</math></i>	970.4(2) / 890.9(2)	2198	117.2(15)	this work
Tl <sub>5</sub> (CO <sub>3</sub> ) <sub>2</sub> (CN)	<i>Cmca</i>	1468.1(3) / 1171.6(2) / 1266.0(3)	2039	109.9(10)	this work

\* Assignment in [5], see comment in text and Fig. 2.

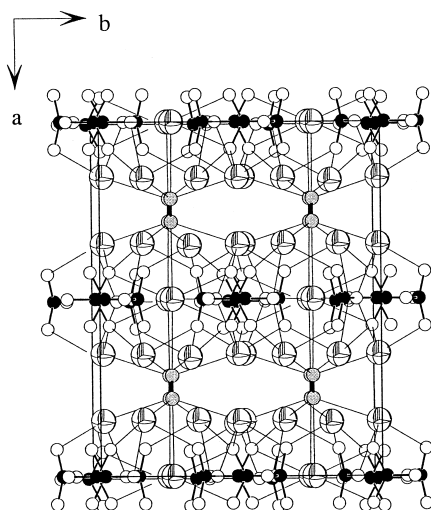


Fig. 3. View along [001] of the unit cell of Tl<sub>5</sub>(CO<sub>3</sub>)<sub>2</sub>(CN). Tl is shown as large white sphere with octahedra drawn, C as black spheres, O as white spheres. The atoms belonging to a cyanide group are displayed as light grey spheres.

Zn(CN)<sub>2</sub> and Cd(CN)<sub>2</sub> both have an *anti*-Cu<sub>2</sub>O structure. This was doubted in a previous paper [8],

and the space group *O $\bar{4}3m$*  (No. 215) was chosen to remove the C/N disorder and to have both atoms on distinguished positions, but the reflection conditions found for Zn(CN)<sub>2</sub> point to either the space group *Pn $\bar{3}$*  (No. 201) or *Pn $\bar{3}m$*  (No. 224).

Hg(CN)<sub>2</sub> has its own structure type with molecular NC-Hg-CN units. Our results corroborate previous results [9].

Tl<sub>5</sub>(CO<sub>3</sub>)<sub>2</sub>(CN) consists of Tl-CO<sub>3</sub>(Tl<sub>3</sub>)CO<sub>3</sub>-Tl layers parallel to the *bc* plane with disordered cyanide anions connecting these layers (Fig. 4).

The carbonate ions have perpendicular orientation to these aforementioned layers and are grouped around Tl3. Tl1 and Tl2 complete the coordination spheres of the carbonate ions, however, both Tl atoms have large voids in their coordination spheres. The voids occur towards the outside of the layer and probably indicate the location of sterically active lone pairs of Tl1 and Tl2. The coordination spheres of all Tl atoms are shown in Fig. 4.

### Final Remarks

The only pseudobinary cyanides which have been shown to be not disordered are LiCN, Hg(CN)<sub>2</sub> and

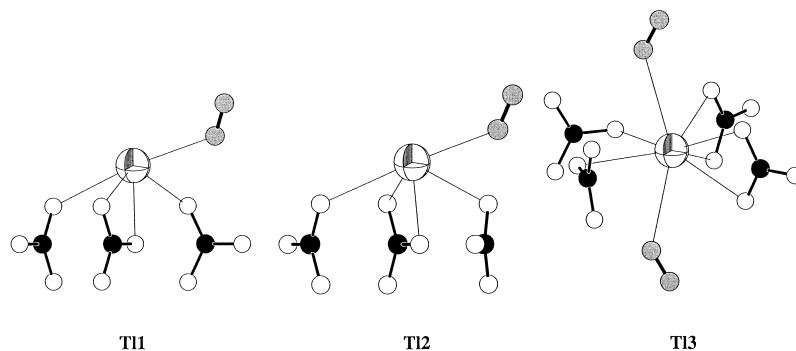


Fig. 4. Coordination spheres of T11, T12 and T13 (left to right) up to 350 pm. The atom representation is as in Fig. 3.

AuCN, but the latter one is probably a similar case as AgCN. Disordered cyanide was also found in the new compound  $Tl_5(CO_3)_2(CN)$ . Because of the similar X-ray scattering power of C and N, X-ray diffraction has limited value in addressing the disorder question. Recently, a study on the structure of AgCN [7] via total neutron diffraction could resolve the disorder problem for this compound.

It is hard to believe that the quest for the structure of a “textbook compound” like CuCN is still not at its successful end, however, this can be considered

as only one example out of many. Only recently Kouvetakis *et al.* [11 - 13] started ‘simple’ cyanide research and provided the first data about alkaline earth metal cyanides which play a role in technical processes and patents.

#### Acknowledgments

We thank Dr. H. Vogt (Max-Planck-Institut für Festkörperforschung) for the Raman measurements as well as Mr. C. Schneck and Prof. Dr. Th. Schleid for the DTA / TG measurements.

- |  |   |
|--|---|
| [1] Program WINXPOW 1.10, Stoe&Cie GmbH, Darmstadt (1999).   | [8] B. F. Hoskins, R. Robson, <i>J. Am. Chem. Soc.</i> <b>112</b> , 1546 (1990).  |
| [2] Program package SHELXTL, G. M. Sheldrick, Göttingen (1997).  | [9] R. C. Seccombe, C. H. L. Kennard, <i>J. Organomet. Chem.</i> <b>18</b> , 243 (1969).  |
| [3] Program package X-SHAPE / X-RED 1.07, Stoe&Cie GmbH, Darmstadt (1996).   | [10] J. A. Lely, J. M. Bijovet, <i>Rec. Trav. Chim. Pays Bas</i> <b>61</b> , 244 (1942).  |
| [4] S. Kroeker, R. E. Wasylshen, J. V. Hanna, <i>J. Am. Chem. Soc.</i> <b>121</b> , 1582 (1999).   | [11] D. J. Williams, B. Pleune, K. Leinenweber, J. Kouvetakis, <i>J. Solid State Chem.</i> <b>159</b> , 244 (2001).   |
| [5] J. Hanawalt, H. Rinn, L. Frevel, <i>Anal. Chem.</i> <b>10</b> , 457 (1938); D. T. Cromer, R. M. Douglass, E. Staritzky, <i>Anal. Chem.</i> <b>29</b> , 316 (1957). | [12] L. C. Brousseau, D. Williams, J. Kouvetakis, M. O’Keeffe, <i>J. Am. Chem. Soc.</i> <b>119</b> , 6292 (1997); D. J. Williams, D. E. Partin, F. J. Lincoln, J. Kouvetakis, M. O’Keeffe, <i>J. Solid State Chem.</i> <b>134</b> , 164 (1997). |
| [6] G. A. Bowmaker, B. J. Kennedy, J. C. Reid, <i>Inorg. Chem.</i> <b>37</b> , 3968 (1998).  | [13] D. Williams, J. Kouvetakis, M. O’Keeffe, <i>Inorg. Chem.</i> <b>37</b> , 4617 (1997).  |
| [7] S. J. Hibble, S. M. Cheyne, A. C. Hannon, S. G. Eversfield, <i>Inorg. Chem.</i> <b>41</b> , 1042 (2002).   |   |